

# The potential use of bacterial community succession in forensics as described by high throughput metagenomic sequencing

Jennifer L. Pechal · Tawni L. Crippen ·  
M. Eric Benbow · Aaron M. Tarone · Scot Dowd ·  
Jeffery K. Tomberlin

Received: 11 March 2013 / Accepted: 7 May 2013  
© Springer-Verlag Berlin Heidelberg 2013

**Abstract** Decomposition studies of vertebrate remains primarily focus on data that can be seen with the naked eye, such as arthropod or vertebrate scavenger activity, with little regard for what might be occurring with the microorganism community. Here, we discuss the necrobiome, or community of organisms associated with the decomposition of remains, specifically, the “epinecrotic” bacterial community succession throughout decomposition of vertebrate carrion. Pyrosequencing was used to (1) detect and identify bacterial community abundance patterns that described discrete time points of the decomposition process and (2) identify bacterial taxa important for estimating physiological time, a time–temperature metric that is often commensurate with minimum post-mortem interval estimates, via thermal

summation models. There were significant bacterial community structure differences in taxon richness and relative abundance patterns through the decomposition process at both phylum and family taxonomic classification levels. We found a significant negative linear relationship for overall phylum and family taxon richness as decomposition progressed. Additionally, we developed a statistical model using high throughput sequencing data of epinecrotic bacterial communities on vertebrate remains that explained 94.4 % of the time since placement of remains in the field, which was within 2–3 h of death. These bacteria taxa are potentially useful for estimating the minimum post-mortem interval. Lastly, we provide a new framework and standard operating procedure of how this novel approach of using

**Electronic supplementary material** The online version of this article (doi:10.1007/s00414-013-0872-1) contains supplementary material, which is available to authorized users.

J. L. Pechal  
Department of Entomology, 2475 TAMU, Texas A&M University,  
College Station, TX 77843, USA

J. L. Pechal (✉)  
Department of Biology, 300 College Park, University of Dayton,  
Dayton, OH 45469-2320, USA  
e-mail: jenpechal18@gmail.com

T. L. Crippen (✉)  
Southern Plains Agricultural Research Center, USDA-ARS,  
2881 F and B Road,  
College Station, TX 77845, USA  
e-mail: tc.crippen@ars.usda.gov

M. E. Benbow (✉)  
Department of Biology, 300 College Park, University of Dayton,  
Dayton, OH 45469-2320, USA  
e-mail: eric.benbow@gmail.com

A. M. Tarone  
Department of Entomology, 2475 TAMU, Texas A&M University,  
College Station, TX 77843, USA  
e-mail: amtarone@tamu.edu

S. Dowd  
Molecular Research LP, 503 Clovis Rd,  
Shallowater, TX 79363, USA  
e-mail: sdowd@mrdnalab.com

J. K. Tomberlin  
Department of Entomology, 2475 TAMU, Texas A&M University,  
College Station, TX 77843, USA  
e-mail: jktomberlin@tamu.edu

high throughput metagenomic sequencing has remarkable potential as a new forensic tool. Documenting and identifying differences in bacterial communities is key to advancing knowledge of the carrion necrobiome and its applicability in forensic science.

**Keywords** Necrobiome · Minimum PMI · Bacteria · Carrion · Decomposition · Epinecrotic communities

## Introduction

One biological component of decomposing vertebrate remains that has received little study for use in minimum post-mortem interval ( $PMI_{min}$ ) estimates is that of the microorganismal communities (e.g., bacteria and fungi), as part of the “necrobiome” as defined by Benbow et al. [1]. The necrobiome is the community of prokaryotic and eukaryotic species associated with decomposing heterotrophic biomass, including animal carrion and human corpses. There are many techniques employed for estimating  $PMI_{min}$  of vertebrate remains. In forensic entomology relative abundance [2], developmental stage [3–5], and succession [6, 7] of arthropod species associated with the remains having been used to estimate a  $PMI_{min}$ . Investigators can assess the decomposition stage of remains and make broad estimations of exposure within a given environment, which can, but does not necessarily, correspond to  $PMI_{min}$  (e.g., remains frozen placed into the environment could skew estimates) [8]. The decomposition process is variable depending on biotic (e.g., scavenging, insect activity) and abiotic (e.g., temperature, barriers preventing access) factors [9]. Vertebrate carrion decomposition is commonly characterized into decomposition stages, ranging from two [7, 10] to eight [11], based on the physical appearance of the remains and associated arthropod arrival patterns. However, regardless of the number of stages, the process from fresh to skeleton stage follows the same sequence. Typically, fresh carrion remains begin to bloat shortly after death due to a proliferation of enteric bacteria. The remains then putrefy and either vertebrate scavengers or necrophilous arthropods consume the soft tissue until the carcass is reduced to bone, cartilage, and any unconsumed tissue or hair.

There has yet to be a study incorporating bacterial communities in estimating carrion decomposition processes and  $PMI_{min}$  in terrestrial ecosystems. There are only a few studies in aquatic systems that used algal and diatom [12], bacterial [13], and fungal communities [14] to predict the post-mortem submersion interval. This lack of production is surprising given the recent technological genomic advances that have made it possible to identify even non-cultural microbial taxa and communities from the environment. Next generation sequencing has led to significant gains in

the knowledge of bacterial communities in decomposition, but has been overlooked in forensic sciences. Massively parallel high throughput sequencing technology, such as pyrosequencing, is based on sequence-by-synthesis theory [15], which generates large amounts of data and obtains sequences for microbial taxa that are new to science and/or unculturable [16, 17]. This technology has been used to characterize bacterial communities in habitats ranging from the human gut [18] to deep mines [19]. Pyrosequencing methods allow for the study of the microbiome in living humans [20], and have demonstrated that humans maintain a high degree of taxon diversity and richness [18, 20–23]. For example, pyrosequencing of microbial samples collected from 27 body regions (e.g., forehead, sole of the foot, oral cavity, and gut) produced 4,949 species-level phylotypes out of a total of 250,000 16S rRNA sequences [24].

In this study, we used pyrosequencing to describe temporal changes during carrion decomposition and to identify members of the epinecrotic communities, which are part of the necrobiome, which had the potential to be useful in  $PMI_{min}$  estimates. We define the epinecrotic community as those organisms residing, or moving, on the surface of decomposing remains, whether it is the skin or mucous membrane of a cavity (e.g., mouth), and is primarily represented by prokaryotes, protists, and fungi. Utilizing high throughput sequencing is a novel approach to characterize bacterial community composition and succession during vertebrate decomposition. Quantifying such change in combination with understanding its relationship with decomposition physiological time ( $h^{\circ}C$ ) could potentially be used to more accurately and reliably estimate the  $PMI_{min}$  for a decedent while accounting for biological variation in such communities. Our objective was to determine how next generation technology could be used to describe bacterial community composition and succession, and to evaluate how such data can be used to make estimates of the  $PMI_{min}$  in death investigations.

There were three goals in this study: (1) describe the epinecrotic bacterial community composition and succession that occurs during decomposition of vertebrate carrion; (2) identify important bacteria taxa from these communities useful in estimating physiological time, which we use as a surrogate of  $PMI_{min}$  estimations; and (3) understand how quantifications of the human necrobiome, and specifically, the epinecrotic communities, over time can potentially be used in forensic investigations.

## Materials and methods

Using replicate swine carcasses ( $n=3$ ) as models of human decomposition [25], we studied the epinecrotic bacterial

community over the course of decomposition in a Midwestern temperate forest habitat surrounded by agricultural fields in Xenia, OH, USA (39.6375° N, 84.0270° W) in August 2010. The dominant tree fauna consisted of oaks (*Quercus* spp.) and maples (*Acer* spp.). The canopy cover was relatively homogeneous (approximately 95 %) over all carcasses [1]. Three male swine ranging from 13.7–30.1 kg, euthanized by cranial blunt force at approximately 16:30 h, were purchased from a local farm on 5 August 2010. Carcasses were double-bagged, transported for approximately 1 h, and randomly placed at least 20 m apart along three transects, as previously described [26], on a flat terrain at approximately 19:00 h on 5 August, which was 2 h before the US National Oceanic and Atmospheric Administration defined sunset. All carcasses were oriented with heads to cardinal north and the dorsal side of the carcass towards the east. Carcasses were covered with anti-scavenging cages (0.9×0.6×0.6 m) constructed of wooden frames enclosed with poultry netting. We categorized decomposition of the remains according to the stages as defined by Payne [6]: fresh, bloat, active decay, advanced decay, and dry. NexSens DS1923 micro-T temperatures loggers (Fondriest Environmental, Inc., Alpha, OH, USA) were placed within 0.6 m of each carcass approximately 0.3 m above the ground and temperature was recorded every 15 min. Temperature data were later converted into physiological time (h °C) using thermal summation models with a base temperature of 0 °C, which accounts for temperature variation over decomposition [27]. This measure is commonly used in forensic applications when extrapolations are made from experimental (i.e., lab) to field data of carrion under different or highly variable thermal environmental conditions [27–29].

#### Bacterial community sampling protocol

Epinecrotic bacterial communities were sampled immediately after carcass exposure in the environment (0) and then at 1, 3, and 5 days thereafter based on preliminary data (not shown). Sterile cotton applicators were used to sample the communities from two regions on each carcass for 60 s: the buccal cavity (the top area of the mouth and under the tongue) and the skin, which consisted of combining three areas (approximately 2.54×15.24 cm) along a single transect of the carcasses, while taking caution not to sample the same areas throughout decomposition. Samples were stored at 4 °C until further processing took place within 12 h of sampling.

#### DNA extraction

DNA extraction took place using a modified chloroform-phenol extraction. Briefly, samples were placed in 1.5-ml microcentrifuge tubes with Tris-EDTA buffer, 10 % SDS,

proteinase K (100 µg/ml), and lysozyme (2 mg/ml). Samples were homogenized and incubated at 56 °C for 1 h while shaken at 900 rpm. Sodium chloride buffer (NaCl, 5 M) was added to bring the total concentration above 0.5 M. Cetyltrimethylammonium bromide/NaCl buffer was added and the sample was thoroughly mixed and incubated at 65 °C for 10 min. Sequential extraction in a ×1 volume was performed using phenol/chloroform/isoamyl alcohol (25:24:1) then chloroform/isoamyl alcohol (24:1). DNA was precipitated with isopropanol by centrifugation at 4,000×g for 2 min, followed by two washes in 70 % ethanol, then dissolved in nuclease-free water, and quantified by NanoDrop spectrophotometer (Nyxor Biotech, Paris, France). DNA products from the three replicate carcasses were mixed in equal concentrations and aliquoted for analysis by pyrosequencing.

#### Pyrosequencing

Bacterial community structure was determined by modified bacterial tagged encoded FLX amplicon pyrosequencing. Extracted DNA from each sample (~100 ng) was sent to the Research and Testing Laboratory (Lubbock, TX). PCR amplification of V1–3 regions of 16S rDNA was performed using the primers for bacterial populations Gray28F (5' TTTGATCNTGGCTCAG) and Gray519r (5'GTNTTAC NGCGGCKGCTG), as previously described [30–33]. Initial generation of the sequencing library occurred with a one-step PCR using a mixture of Hot Start and HotStar high-fidelity *Taq* polymerases. PCR clean-up was performed with an UltraClean® PCR Clean-Up Kit (MO BIO Laboratories, Inc. Carlsbad, CA). Amplicons were obtained from the Gray28F for bacterial diversity. A Roche 454 FLX instrument with Titanium reagents and Titanium procedures were employed to perform the tag-encoded FLX amplicon pyrosequencing analyses based on RTL protocols ([www.researchandtesting.com](http://www.researchandtesting.com)). The sequences have been deposited in the Sequence Read Archive at EBI with study accession number ERP001998.

#### Pyrosequencing data analysis

Following sequencing, all failed sequence reads, low-quality sequence ends, and tags and primers were removed, and sequences depleted of any non-bacterial ribosome sequences and chimeras using B2C2 [34], as previously described [35–39]. Sequences were aligned, using the Ribosomal Database Project (RDP) under tool Aligner (accessed on September 27, 2012), based on the 16S rRNA secondary structure in Infernal aligner [40, 41]. Taxonomic classification of 16S rRNA sequences were performed using Naïve Bayesian rRNA classifier version 2.2 in RDP (accessed on September 27, 2012) according

to Bergey's bacterial taxonomy [42, 43]. Only sequences having  $\geq 80$  % bootstrap support were considered classified at a given taxonomic rank (phylum to family). Bacterial taxon richness and relative abundance was determined for each sampling region (i.e., buccal and skin) at each taxonomic rank. "Rare taxa" represented those with  $< 3$  % of total abundance.

### Bacterial community analyses

Bacterial communities were analyzed at both phylum and family taxonomic resolutions as defined by Wang et al. [43]. Taxon richness was analyzed using linear regression over physiological time. Physiological time ( $h^{\circ}C$ ) was calculated by summing average daily temperature over the course of the study. Because we were only interested in how bacterial communities (not insects) changed with physiological time,  $0^{\circ}C$  minimum threshold was employed in this calculation. Many bacterial species that cannot be cultured continue to grow and reproduce even under cold temperatures, thus, making a minimum threshold estimate difficult for community data. To further analyze differences in taxon richness, permutational multivariate analysis of variance (PERMANOVA) was tested using the *adonis* function in the *vegan* 2.0–3 library in the R statistical package [44, 45]. PERMANOVA is a nonparametric technique used to differentiate groups based on a Bray–Curtis dissimilarity matrix [45]. Bray–Curtis distance with nonmetric multidimensional scaling (NMDS) using the *vegan* library in the R statistical package and PC-ORD 5 (MjM Software, Gleneden Beach, OR, USA) [46] was used to analyze operational taxonomic units, determined in the pyrosequencing analyses, over decomposition. NMDS is a nonparametric ordination technique that avoids assuming linearity among community variables [47]. Multi-response permutation procedure (MRPP) in PC-ORD 5 was employed for testing statistical differences between covariates (i.e., decomposition day and region of sampling) of bacterial community composition within the ordination using methods described elsewhere [48]. Indicator species analysis (ISA) in PC-ORD 5 complemented MRPP by assigning significant indicator values to bacteria taxa (phylum or family) that were indicative of community structure separation between sampling regions (i.e., buccal and skin) and over decomposition after Bonferroni corrections [47]. We used indicator values to identify bacterial taxa that best represented communities of each sampling region and during decomposition based on phylum or family classification, with 0 representing no indication and 100 being a perfect indication of each grouping [47].

A tiered statistical approach was used to estimate decomposition time, as determined from physiological time, using bacterial community composition. Random forest models were used to identify taxa that contributed most to variation in physiological time. The highest-ranking predictor taxa

from the random forest algorithm were then evaluated as factors that significantly varied over time as measured by physiological time using either generalized additive models (GAMs) or generalized linear models (GLMs). Random forest models were constructed using the *randomForest* 4.6–6 library in the R statistical package [44]. The *mgcv* 1.7–13 library in the R statistical package [44] was used to construct both GAMs and GLMs. Evaluation of the models was performed using a Gaussian distribution with an identity link function as determined from residuals plots of the model. Using a combination of either indicator taxa from ISA or taxa identified in the random forest analysis we constructed competing models that used bacterial taxa to estimate physiological time [49]. Because bacteria can survive within a wide range of temperatures, even demonstrating growth below freezing [50], bacterial growth was presumed to be associated with decomposition under the environmental temperature ranges of this study. This assumption was based on reported understanding of psychrotrophic and mesophilic bacteria [51], which were common in this study and were not expected to grow in freezing conditions. Since the bacterial communities identified in the study belonged to these well-described communities, a minimum base temperature of  $0^{\circ}C$  was assumed for these analyses.

## Results

### Decomposition progression

The local mean daily ambient temperature among carcasses was  $23.2 \pm 2.1^{\circ}C$  and physiological time ( $h^{\circ}C$ ) increased linearly throughout decomposition (Fig. S1). Fresh stage began at time of death ( $0 \pm 0 h^{\circ}C$ ) with no odor emitted, no visual indication of decomposition and no observed arthropod colonization. Bloat stage occurred within 24 h ( $544 \pm 3 h^{\circ}C$ ) of field placement and was characterized by expansion of the body torso with color changes resulting from tissue marbling associated with gas accumulation. Calliphorid eggs were documented in large masses on the head of each carcass. Active decay stage was indicated by soft tissue removal by Calliphoridae (from eggs to third instars) with the remainder of the carcass beginning to deflate on the third day ( $1,540 \pm 5 h^{\circ}C$ ). All larval activity was primarily located on the head region. Advanced decay stage was documented on the fourth day of decomposition ( $2,780 \pm 4 h^{\circ}C$ ) and was similar to the active decay stage, but most soft tissue had been removed by calliphorid larval masses (potentially thousands of larvae as a collective aggregation) [26]. Carcasses decomposed to the dry stage, which represented the end of decomposition with no soft tissue remaining and calliphorid larvae dispersing from the



resource, between the sixth ( $3,308 \pm 16$  h °C) and seventh day ( $3,912 \pm 19$  h °C) of decomposition.

#### Epinecrotic bacterial community composition during decomposition

The bacterial communities demonstrated marked differences in taxon richness and relative abundance patterns through the decomposition process at both phylum and family taxonomic classification levels. Carcasses decomposition to the dry stage occurred within 5 days ( $2,692$  h °C) of field placement, and each decomposition stage had a unique profile of 4 dominant bacteria community phyla and 20 families that changed during carrion decomposition.

#### Phylum level taxonomic resolution

A total of 137,181 sequences were obtained throughout decomposition from the samples of all three carcasses combined. There were notable trends and changes in bacterial taxon relative abundance, excluding rare taxa (<3 % relative abundance), at phylum level throughout decomposition (Fig. 1, Table S2). Over the course of decomposition (via h °C), Proteobacteria was the dominant phylum ( $70.4 \pm 1.6$  %) with Firmicutes being the next most abundant, representing  $20.1 \pm 6.6$  % of the community. Proteobacteria decreased over time, changing from the dominant phylum

on the first ( $41.9 \pm 10.3$  %) and third ( $30.9 \pm 44.9$  %) days to only  $2.5 \pm 2.2$  % by the fifth day. Firmicutes became the dominant taxon as decomposition progressed comprising of  $36.2 \pm 9.6$ ,  $57.3 \pm 38.6$ , and  $96.6 \pm 1.3$  % on the first, third, and fifth sampling day, respectively. Rare phyla accounted for less than 0.5 % of the total relative abundance across decomposition (Fig. 1).

There was a significant negative linear relationship of phylum taxon richness over the course of decomposition (Fig. 2). Phylum richness decreased by 30.6 % ( $y = -0.007x + 5.95$ ,  $R^2 = 0.40$ ,  $P = 0.0002$ ) when all phyla were included and by 53.6 % when rare phyla (<3 % relative abundance) were removed ( $y = -0.001x + 2.94$ ,  $R^2 = 0.53$ ,  $P < 0.0001$ ).

At phylum level, there was a significant difference in the epinecrotic bacterial communities among sampling days, but there was no significant differences among replicate carcasses, nor were there significant interactions (Table S3, S4). A two-dimensional NMDS ordination explained 95.6 % (stress=0.11) of bacterial community structure (Fig. S2) with significant differences between the earliest days of decomposition and the last day (Table S5).

Fusobacteria was a significant indicator phylum of the overall epinecrotic community on the first sampling day, while Actinobacteria significantly represented the skin communities (Table S5). There were no other significant indicator phyla. Five phyla were determined to be important predictors of estimating physiological time from random

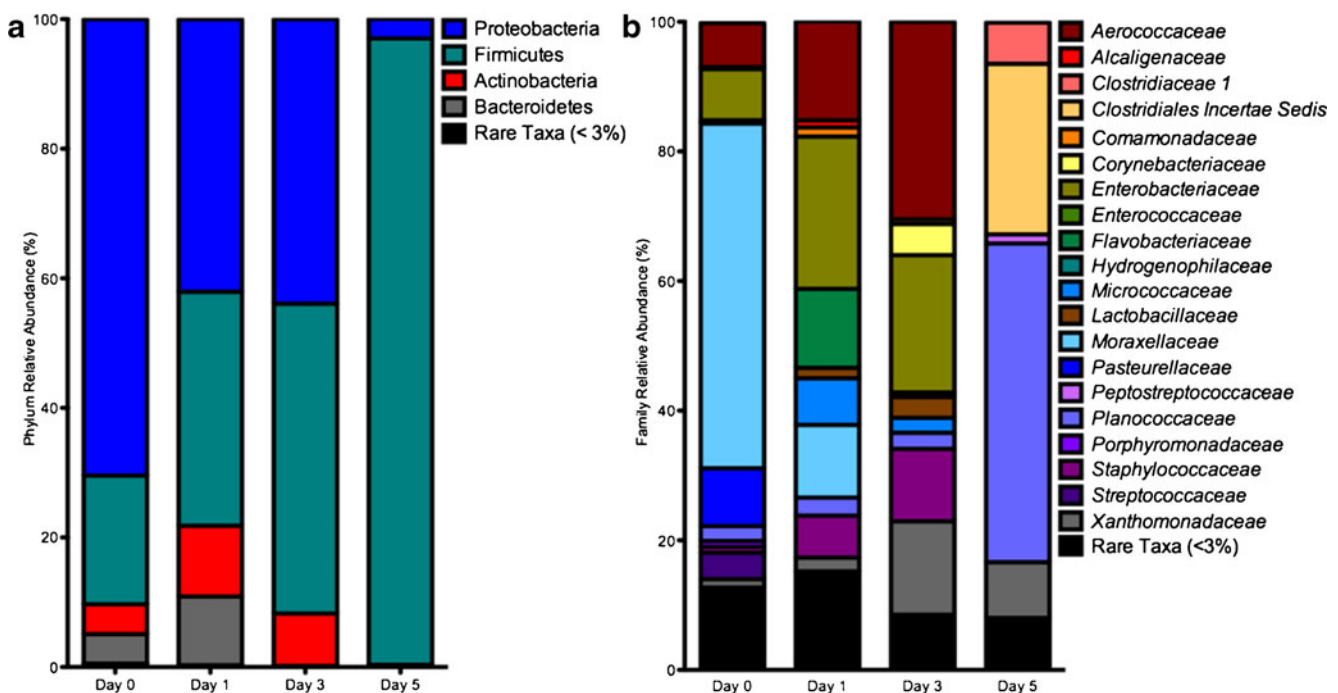


**Fig. 1** Bacterial community-relative abundance at **a** phylum and **b** family taxonomic level with rare taxa cut off at <3 % relative abundance on decomposing swine carcasses. Carcasses transitioned from

fresh (initial placement–0 h °C) to bloat (Day 1–541 h °C) to active decay (Day 3–1,535 h °C) to dry (Day 5–2,692 h °C) decomposition within 5 days of placement in the field

forest analyses, and explained 62.1 % of the variation in physiological time throughout decomposition (Fig. S3).

### Family level taxonomic resolution

Over the course of decomposition, *Moraxellaceae* was the most dominant ( $51.3 \pm 23.2$  %) with *Pasteurellaceae*, *Enterobacteriaceae*, and *Aerococcaceae* representing  $8.9 \pm 4.9$ ,  $7.9 \pm 13.8$ , and  $6.8 \pm 3.0$  % relative abundance, respectively (Fig. 1, Table S2). On the first sampling day (Fig. 1, Table S2), *Moraxellaceae* was reduced ( $11.2 \pm 5.5$  %) and was not present on either the third or fifth sampling day. However, *Aerococcaceae* increased throughout decomposition until the third sampling day and then was not present on the fifth day. *Enterobacteriaceae* followed a similar trend increasing in relative abundance until the third day of decomposition with no presence after 5 days. *Planococcaceae* was the most dominant family ( $49.2 \pm 12.3$  %) on the fifth day (Fig. 1, Table S2),

which was about a 20-fold increase from the previous three sampling time points. The next two dominant families on the fifth day were *Clostridiales incertae sedis* XI ( $26.3 \pm 17.2$  %) and *Clostridiaceae* ( $6.4 \pm 8.2$  %). Rare families accounted for 12.7, 15.2, 8.5, and 8.0 % of the total relative abundance on initial placement and 1, 3, and 5 days of decomposition, respectively (Fig. 1).

There was a significant negative linear relationship for overall family taxon richness over the course of decomposition (Fig. 2). Family richness decreased 60.2 % by the end of the fifth sampling day ( $y = -0.010x + 44.41$ ,  $R^2 = 0.74$ ,  $P < 0.0001$ ), but only decreased by 17.5 % when rare taxa were removed ( $y = -0.0003x + 4.10$ ,  $R^2 = 0.049$ ,  $P = 0.3071$ ).

There was a significant difference in the epinecrotic bacterial community among days, with no significant differences among replicate carcasses or significant interactions; however, there was a significant difference between

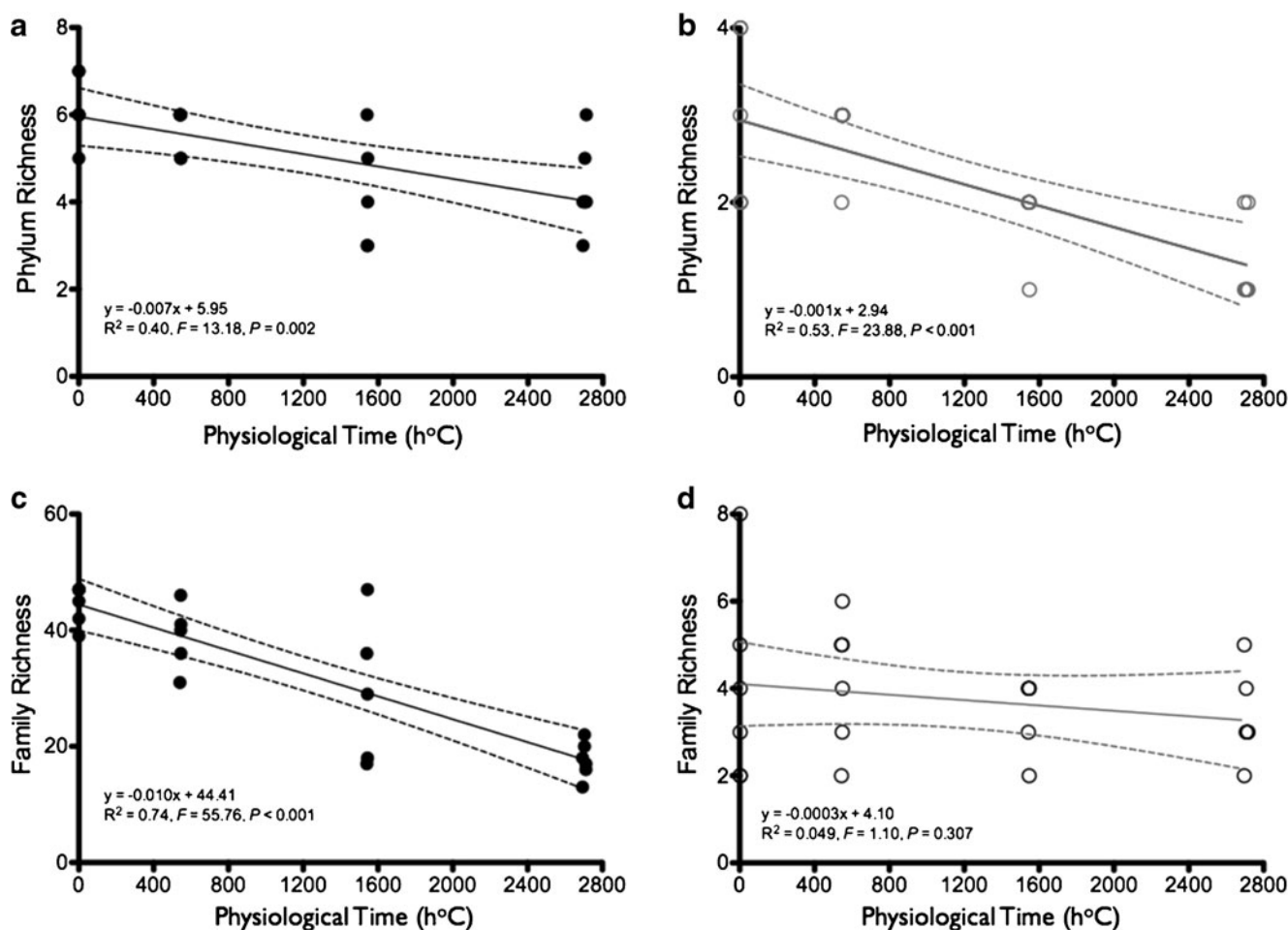


**Fig. 2** Taxon richness of bacterial communities decreased linearly over decomposition (h°C). Phylum richness decreased by **a** 30.6 % when all taxa were present ( $y = -0.007x + 5.95$ ,  $R^2 = 0.40$ ,  $P = 0.0002$ ) and **b** 53.6 % when rare taxa were removed ( $y = -0.001x + 2.94$ ,  $R^2 = 0.53$ ,  $P < 0.0001$ ). Family richness decreased by **c** 60.2 % when all taxa were present ( $y = -0.010x + 44.41$ ,  $R^2 = 0.74$ ,  $P < 0.0001$ ), however,

once rare taxa were removed richness decreased **d** by only 17.5 % ( $y = -0.0003x + 4.10$ ,  $R^2 = 0.049$ ,  $P = 0.3071$ ). Each **dark filled circle** (all taxa present) and **light filled circle** (rare taxa removed) represent the bacterial community of a single sampling region (i.e., head or skin region) from an individual carcass;  $n = 6$  for each sampling time point (h°C). The dotted lines represent the 95 % confidence intervals

sampling regions (i.e., buccal and skin bacterial communities) and a significant interaction effect with sampling day (Table S7, S8). A two-dimensional NMDS ordination explained 75.2 % (stress=0.24) of bacterial community structure at the family taxonomic level (Fig. S2) with significantly different epinecrotic communities among sampling days (MRPP:  $T=-5.50$ ,  $P < 0.0001$ ). Pair-wise comparisons indicated significant differences in bacterial community composition between all pairs of sampling days (initial placement, 1, 3, and 5 days) except between initial placement and day 1, and days 1 and 3 (Table S5).

There were 17 indicator families across decomposition (Table S9). However, after Bonferroni correction (adjusted  $\alpha=0.0029$ ) there were only four significant indicators of decomposition. During the initial sampling, *Bacteroidaceae* and *Moraxellaceae* were significant indicators, while *Bacillaceae* and *Clostridiales Incertae Sedis* XI were significantly represented the communities after on sampling day 5. There were three indicator families representing the skin communities before Bonferroni correction (Table S9). Ten families were determined to be important for estimating physiological time from random forest analyses and explained 78.5 % of the variation in physiological time throughout decomposition (Fig. S4).

#### Models estimating significant predictors of physiological time

Using indicator phyla or families from either ISA or random forest analysis we developed models that best described variation in physiological time. The ISA significant indicator taxon (*Fusobacteria*) provided the poorest model for estimating physiological time (15.1 % of the variation; Table 1). The full model using all five phyla from the

random forest analysis explained 84.1 % (generalized cross-validation score ( $GCV$ )=4.60e+05) of the variation in physiological time (Table 1). However, there were four phyla from the random forest analysis that provided the best model and explained the most variation in physiological time (84.4 %,  $GCV$ =4.16e+05). Those four phyla were: Bacteroidetes, Proteobacteria, Actinobacteria, and Firmicutes. These phyla showed substantial shifts in relative abundance over decomposition (Fig. 1).

Significant epinecrotic family indicators from the ISA results provided the best models for estimating physiological time (Table 2). The full model using 17 families identified from random forest explained 96.0 % (Akaike information criterion ( $AIC$ )=345.3) of physiological time variation, while a reduced model with only 10 taxa (Table 2) was the most informative and explained the most amount of variation in physiological time (94.4 %,  $AIC$ =343.2). At family level of identification, the taxa identified by random forest analyses produced the poorest models (Table 3) explaining 62.3–92.3 % in physiological time variation. Overall, family level taxa from indicator species analysis produced the best model for explaining the variation in physiological time.

#### Discussion

We developed a model using high throughput metagenomic sequencing of bacterial communities on vertebrate remains that explained 94.4 % of the time since placement of remains in the field (as measured by physiological time), which was within 2–3 h after death. Ambient air temperatures were consistent across carcasses since the remains were located in the same habitat and thus physiological time

**Table 1** Generalized additive models estimating physiological time (h °C) using bacteria community phyla indicators from either random forest or indicator species analysis results

Model	Indicator taxa source	Physiological time (h °C) =	R <sup>2</sup> (adj.)	Percent (%)	GCV
1	Random forest	s(Bacteroidetes) + s(Proteobacteria) + s(Actinobacteria) + s(Firmicutes) + s(Fusobacteria)	0.754	84.1	4.60e+05
2	Random forest	s(Bacteroidetes) + s(Proteobacteria) + s(Actinobacteria) + s(Firmicutes)	0.768	84.4	4.16e+05
3	Random forest	s(Bacteroidetes) + s(Proteobacteria) + s(Actinobacteria)	0.709	78.5	4.75e+05
4	Random forest	s(Bacteroidetes) + s(Proteobacteria)	0.430	50.5	7.91e+05
5	Random forest	s(Bacteroidetes)	0.154	20.9	1.09e+06
6	ISA	s(Fusobacteria)	0.088	15.1	1.18e+06

Each model is accompanied by the R<sup>2</sup> (adj.) value, the percent variation of physiological time (%) explained by each model and the generalized cross-validation score (GCV), in which a lower value indicates a better model

**Table 2** Generalized linear models estimating physiological time (h °C) using bacteria community family indicators from the indicator species analysis results

Model	Indicator taxa source	Physiological time (h °C) =	Percent (%)	AIC
11	ISA	<i>Campylobacteraceae</i> + <i>Enterococcaceae</i> + <i>Prevotellaceae</i> + <i>Moraxellaceae</i> + <i>Hyphomicrobiaceae</i> + <i>Clostridiales Incertae Sedis XI</i> + <i>Porphyromonadaceae</i> + <i>Pasteurellaceae</i> + <i>Bacillales Incertae Sedis XI</i> + <i>Brucellaceae</i> + <i>Neisseriaceae</i> + <i>Rhodocyclaceae</i> + <i>Streptococcaceae</i> + <i>Fusobacteriaceae</i> + <i>Bacteroidaceae</i> + <i>Xanthomonadaceae</i> + <i>Bacillaceae</i> 2	96.0	345.3
12	ISA	<i>Campylobacteraceae</i> + <i>Enterococcaceae</i> + <i>Prevotellaceae</i> + <i>Moraxellaceae</i> + <i>Hyphomicrobiaceae</i> + <i>Clostridiales Incertae Sedis XI</i> + <i>Porphyromonadaceae</i> + <i>Pasteurellaceae</i> + <i>Bacillales Incertae Sedis XI</i> + <i>Brucellaceae</i> + <i>Neisseriaceae</i> + <i>Rhodocyclaceae</i>	94.8	345.3
13	ISA	<i>Campylobacteraceae</i> + <i>Enterococcaceae</i> + <i>Prevotellaceae</i> + <i>Moraxellaceae</i> + <i>Hyphomicrobiaceae</i> + <i>Clostridiales Incertae Sedis XI</i> + <i>Porphyromonadaceae</i> + <i>Pasteurellaceae</i> + <i>Bacillales Incertae Sedis XI</i> + <i>Brucellaceae</i>	94.4	343.2
14	ISA	<i>Campylobacteraceae</i> + <i>Enterococcaceae</i> + <i>Prevotellaceae</i> + <i>Moraxellaceae</i> + <i>Hyphomicrobiaceae</i> + <i>Porphyromonadaceae</i> + <i>Pasteurellaceae</i> + <i>Bacillales Incertae Sedis XI</i> + <i>Brucellaceae</i>	92.9	346.3

Each model is accompanied by the percent variation of physiological time (%) explained by each model and the Akaike information criterion (AIC), which was used to select the best model

was equivalent to temporal age (Fig S1). Frequently in forensic entomology, physiological time calculated by thermal summation models is estimated from developmental data sets where temperature was stable (i.e., laboratory studies) for each replicate [3–5]. We are not aware of other

empirical studies in forensics that provide a tool for estimating physiological time, as a surrogate of PMI<sub>min</sub>, using bacterial communities. Previous studies examining decomposition have primarily focused on larger-scale observable data such as insects [52] or vertebrate scavengers [53] with

**Table 3** Generalized additive models estimating physiological time (h °C) using bacteria community family indicators from random forest results

Model	Indicator taxa source	Physiological time (h °C) =	R <sup>2</sup> (adj.)	Percent (%)	GCV
1	Random forest	s( <i>Campylobacteraceae</i> ) + s( <i>Moraxellaceae</i> ) + s( <i>Aerococcaceae</i> ) + s( <i>Micrococcaceae</i> ) + s( <i>Clostridiales Incertae Sedis XI</i> ) + s( <i>Comamonadaceae</i> ) + s( <i>Fusobacteriaceae</i> ) + s( <i>Veillonellaceae</i> ) + s( <i>Lachnospiraceae</i> ) + s( <i>Neisseriaceae</i> )	0.817	91.3	4.61e+05
2	Random forest	s( <i>Campylobacteraceae</i> ) + s( <i>Moraxellaceae</i> ) + s( <i>Aerococcaceae</i> ) + s( <i>Micrococcaceae</i> ) + s( <i>Clostridiales Incertae Sedis XI</i> ) + s( <i>Comamonadaceae</i> ) + s( <i>Fusobacteriaceae</i> ) + s( <i>Veillonellaceae</i> ) + s( <i>Lachnospiraceae</i> )	0.827	91.4	4.19e+05
3	Random forest	s( <i>Campylobacteraceae</i> ) + s( <i>Moraxellaceae</i> ) + s( <i>Aerococcaceae</i> ) + s( <i>Micrococcaceae</i> ) + s( <i>Clostridiales Incertae Sedis XI</i> ) + s( <i>Comamonadaceae</i> ) + s( <i>Fusobacteriaceae</i> ) + s( <i>Veillonellaceae</i> )	0.841	91.6	3.60e+05
4	Random forest	s( <i>Campylobacteraceae</i> ) + s( <i>Moraxellaceae</i> ) + s( <i>Aerococcaceae</i> ) + s( <i>Micrococcaceae</i> ) + s( <i>Clostridiales Incertae Sedis XI</i> ) + s( <i>Comamonadaceae</i> ) + s( <i>Fusobacteriaceae</i> )	0.851	92.3	3.46e+05
5	Random forest	s( <i>Campylobacteraceae</i> ) + s( <i>Moraxellaceae</i> ) + s( <i>Aerococcaceae</i> ) + s( <i>Micrococcaceae</i> ) + s( <i>Clostridiales Incertae Sedis XI</i> ) + s( <i>Comamonadaceae</i> )	0.836	90.2	3.33e+05
6	Random forest	s( <i>Campylobacteraceae</i> ) + s( <i>Moraxellaceae</i> ) + s( <i>Aerococcaceae</i> ) + s( <i>Micrococcaceae</i> ) + s( <i>Clostridiales Incertae Sedis XI</i> )	0.847	90.2	2.90+05
7	Random forest	s( <i>Campylobacteraceae</i> ) + s( <i>Moraxellaceae</i> ) + s( <i>Aerococcaceae</i> ) + s( <i>Micrococcaceae</i> )	0.745	81.8	4.30e+05
8	Random forest	s( <i>Campylobacteraceae</i> ) + s( <i>Moraxellaceae</i> ) + s( <i>Aerococcaceae</i> )	0.763	79.4	4.08e+05
9	Random forest	s( <i>Campylobacteraceae</i> ) + s( <i>Moraxellaceae</i> )	0.740	78.5	3.81e+05
10	Random forest	s( <i>Campylobacteraceae</i> )	0.587	62.3	5.44e+05

Each model is accompanied by the R<sup>2</sup> (adj.) value, the percent variation of physiological time (%) explained by each model and the generalized cross-validation score (GCV), which a lower value indicates a better model



little regard for what might be occurring with the microbial communities; despite implications of the microbial community function in key decomposition processes (e.g., volatile organic compound production) [54, 55]. No experiment can a priori account for temperature fluctuations throughout larval development, therefore forensic practitioners use, and expect, physiological time values (e.g., h °C or ADH) [8]. It is clear from our data that there are temporally distinct bacterial communities over time as decomposition visually progresses (e.g., fresh vs. advanced decay). However, we found the ability to differentiate bacterial communities throughout physiological time depends on the level of taxonomic resolution.

We documented how using high throughput metagenomic sequencing can describe the epinecrotic bacterial communities of the necrobiome in a way that is possible to estimate the stages of carrion decomposition, but that this ability was dependent on the taxonomic scale of resolution. Interestingly, all non-rare taxa (>3 % relative abundance) have been documented in the human microbiome [20, 56–59]. Other microorganisms present on a carcass as decomposition progresses such as fungus [60], or bacteria transported to a carcass or corpse via flies, could be affecting taxon richness through processes like competition [61, 62]. Additionally, the decrease in taxon richness over time could result from insect colonization and utilization of the remains. Insect colonizers (e.g., blow flies and necrophilous or necrophagous beetles) use carrion as a nutrition source, mating or oviposition site. Subsequent larval development may disrupt established microbial communities through direct or indirect competitive interactions on the carcass. Insects have many strategies for combating microbial communities including initiating immune responses after pathogen detection [63–65], pathogen avoidance as seen in honey bee colonies rejecting nest mates whom have been infected or parasitized [66, 67], and insects producing secretions containing antibiotic properties [68–70]. Blow flies may directly impact microbial species through chemical secretions while consuming carrion tissue [71, 72].

Additionally, blow flies may be using bacterial quorum sensing communication as signals for arrival patterns and behavior such as oviposition [73, 74]. Further analysis is needed to determine how changes in the bacterial community structure alter insect arrival and colonization patterns of carrion once microbial proliferation has occurred. This information could also be useful in estimating the PMI<sub>min</sub> using the necrobiome either with insects or microbes, and especially useful in instances where insects do not immediately colonize the remains. However, the base temperature utilized in our study would not be appropriate for those bacteria in other categories occurring outside of the 0 °C (our base temperature applied in this study) and 60 °C range. We

selected 0 °C as our base temperature as it was well below the minimum temperature experienced in our study and would represent a minimum temperature that would support the bacteria identified in our study. Since the base temperature influences the slope associated with the physiological time, selection of an erroneous base temperature could result in an over or under estimation of the degree of accuracy of the resulting model for predicting a PMI<sub>min</sub>. Future research should examine the microbial communities that are stable on carrion as it decomposes over time and determine specific ranges of base temperatures that would allow for the refinement and increased accuracy of our model. Without knowing the true base temperatures of the microbial communities identified in this study, our model is a starting point of investigation, which will be improved as more details regarding bacterial base temperatures are determined from empirical studies.

We demonstrate with this study that understanding differences in carrion, or human, epinecrotic bacterial communities is important for advancing knowledge of the necrobiome and its applicability in forensics. Specifically, we provide some of the first empirical evidence that bacterial communities can be used to estimate physiological time as a surrogate of decomposition. A tiered approach using GAMs and GLMs was employed to assess if coarse-scale indicator taxa (i.e., results from ISA representing physiological time throughout decomposition) or fine-scale indicator taxa (i.e., results from random forest analysis) would be best for estimating physiological time. Accuracy of GAMs to predict blow fly age in association with developmental and gene expression data has been examined in previous forensic research [75, 76].

Using phylum level data, random forest indicator phyla explained 92.3 % of the variation in physiological time, but ISA indicator taxa at the family level explained the overall greatest amount of variation (94.4 %) in physiological time. However, one must keep in mind that overfitting is always possible with multivariate models. The addition of a term (e.g., bacteria taxon) must overcome the natural increase in precision expected by adding an additional covariate, and thus, adding a term must improve a model considerably to make it worth keeping or one risks making predictions with a model that is not generalizable [49]. Ultimately, the parameters identified here can be utilized in alternative statistical methods (e.g., inverse prediction models) to determine PMI<sub>min</sub> estimates in the future [77]. Any such model would need to be tested in field conditions, thus blind testing of these models is necessary for validation [49]. If blind studies fail to validate the models then additional environmental observations are required and a recommendation for regional-, local- and seasonal-models would be warranted.

Depending on the scale of information required in an investigation, there are two approaches using epinecrotic

bacteria community data to be useful in estimating a  $PMI_{min}$ . We found that phylum level taxonomic resolution was best to distinguish between days of decomposition. But family level indicator taxa were best at estimating variation in physiological time, a finer temporal scale surrogate for decomposition time. The approach of using bacteria community data is similar to  $PMI_{min}$  estimates using blow fly development data. There are numerous data sets available for blow fly development at constant temperatures [76, 78–80], which are then used to estimate a  $PMI_{min}$ .

### Using epinecrotic communities in forensic investigations

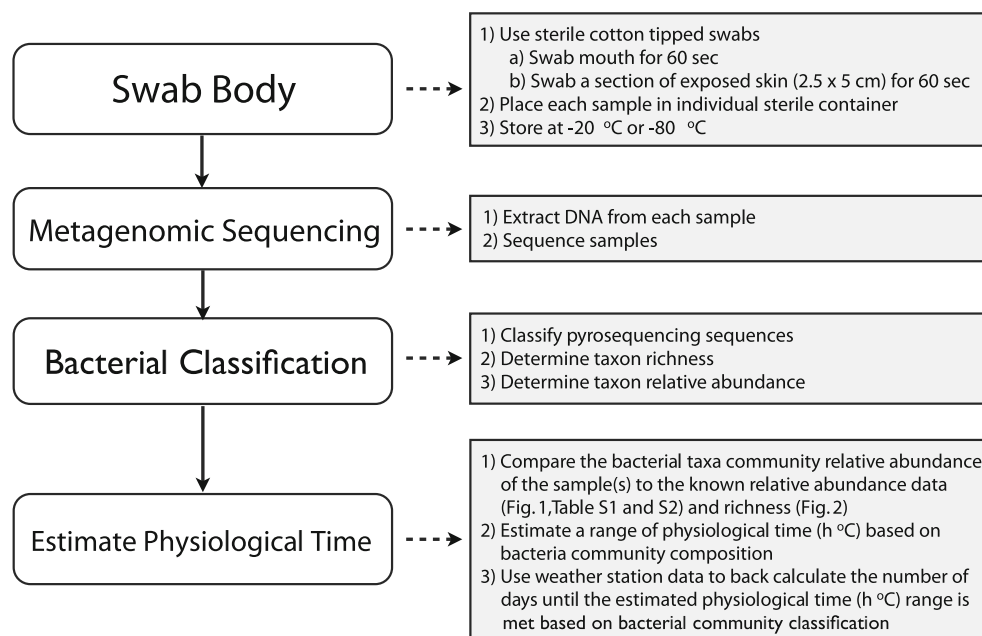
With the documentation of bacterial succession over decomposition and evidence of estimating physiological time from bacterial taxa, the following question arises: How useful will these data be in a forensic application? Therefore, we propose a framework (Fig. 3) of how epinecrotic bacterial community data would be used in casework. Once remains have been located, investigators would swab the buccal and skin using sterile cotton-tipped swabs. This approach would provide the crime scene evidence collection that could be used to describe an overall bacterial community profile of the remains at time of discovery. Samples are then stored individually in separate containers and placed at  $-20^{\circ}\text{C}$  until further analysis. Metagenomic sequencing is performed once the DNA from each sample has been extracted and processed for sequencing (as described in this paper).

High throughput sequencing techniques currently available are pyrosequencing and Illumina with new techniques continuously being developed (e.g., ion torrent).

For this study, pyrosequencing was the preferred sequencing method; however, as technologies improve, there may be more efficient and cost-effective sequencing approach for detecting and identifying bacterial communities. After sequencing, the sequences must be classified and the overall bacterial community assessed by determining taxon richness and relative abundance at the preferred level of taxonomic resolution. These data are necessary for the final step of estimating the number of days of decomposition or the physiological time. Bacterial communities from samples are then compared to reference data from similar environments, such as those of this study, including taxon richness and relative abundance. The bacterial community-relative abundance can be compared to the known ratios of dominant taxa across decomposition (Fig. 1). Finally, data from the nearest weather station can be collected and used to back calculate the estimated physiological time range based on bacterial communities. However, there is a caveat with this approach since the reference data have an upper threshold of approximately 3,000 h at approximately  $23^{\circ}\text{C}$  during decomposition of swine remains. However, insect activity usually occurs within this temperature range and represents a quantified method for estimating time of colonization and thus a  $PMI_{min}$ .

The approach of this framework is similar to methods used by forensic entomologists. For example, insect samples collected on remains can be compared to known development data sets with established physiological time ranges

**Fig. 3** Framework for utilizing bacterial communities to estimate physiological time ( $h^{\circ}\text{C}$ )



associated with each insect development stage. Physiological time estimates based on thermal summation models can then be provided based on temperature data collected from a weather station in the surrounding area. As opposed to growth rates of specific bacterial taxa, we are suggesting that overall abundance or relative abundance of specific taxa, within the epinecrotic community can estimate physiological time and thus the PMI<sub>min</sub>. These bacterial communities are functioning partly as would gene expression levels in blow fly analyses [81] and partly as succession data [82]. This would be a productive avenue for future studies.

There are limitations to the reference data set provided in this paper. Despite the wealth of information provided by pyrosequencing, a lack of known reference genomes for sequence comparisons, an increased error rate with sequencing insertions–deletions, and the expense of utilizing the technology current limits its widespread use in forensics [83]. Additionally, computation limitations of pyrosequencing include cost, the need for sufficient computing power, and limitations in algorithms capable of analyzing the output in a biologically relevant manner [16, 23]. Due to the novel approach of this forensic method, more data is needed to further account for variation in epinecrotic bacterial communities associated with human remains in different habitats, geographic regions, and seasons. The spatial and temporal differences in bacteria communities could be analogous to insects of forensic importance where a single blow fly species, e.g., *Cochliomyia macellaria* (Fabricius) (Diptera: Calliphoridae), demonstrates variation in development among geographic regions [84, 85] and ambient temperature regimes [4, 86].

Although done in one location and one season in Ohio, to the best of our knowledge, this study documents for the first time a metagenomic approach to analyze distinct bacterial communities throughout carrion vertebrate decomposition and the potential use of bacterial communities to estimate physiological time with decomposing vertebrate remains (e.g., human). We advocate for future studies to use this proposed framework in other biomes and during different seasons to add to a larger database with the potential to use bacterial communities in estimating the PMI<sub>min</sub> of carcasses or corpses, in a range of environmental conditions. Additionally, our study demonstrates how epinecrotic community structure can be used to discriminate decomposition time via both simple (e.g., relative abundance) and sophisticated modeling (i.e., GAMs and GLMs) approaches. Epinecrotic bacterial communities had distinct profile shifts within 1 day of decomposition, and this may prove useful in scenarios where other forensic evidence is lacking: for example, when forensically important insects have not yet colonized the remains at the time of discovery. There is tremendous potential in the future for utilizing epinecrotic bacterial communities as a tool in forensics. Additionally, these data contribute to the growing

knowledge base of the overall dynamics of the necrobiome and decomposition ecology. The linkage of the necrobiome to decomposition ecology could identify critical community interactions important to the decomposition process, mechanisms governing attraction of non-microbes to carrion, and effects of the decomposition processes in nature along with forensic relevance and potential application.

**Acknowledgments** We thank A. Lewis, T. Blair, and J. White for their help during the study. The Blair family is gratefully acknowledged for allowing access to their property for this research. We thank B. Singh for assistance in the metagenomic data sequence classification processing. Financial support was given to JLP from the Department of Entomology and the Whole Systems Genome Initiative at Texas A&M University. AMT and JKT would like to thank the Department of Entomology at Texas A&M University and Texas A&M University AgriLife Research for financial support of this project. MEB was supported by the University of Dayton Research Council and the Department of Biology.

**Disclaimer** This project was funded (TLC, MEB, AMT, and JKT), in part, by the National Institute of Justice, Office of Justice Programs, US Department of Justice through Grant 2010-DN-BX-K243. Points of view in this document are those of the authors and do not necessarily represent the official position or policies of the U.S. Department of Justice. Mention of trade names, companies, or commercial products in this publication is solely for the purpose of providing specific information and does not imply recommendation or endorsement of the products by the US Department of Agriculture

## References

1. Benbow M, Lewis A, Tomberlin J, Pechal J (2013) Seasonal necrophagous insect community assembly during vertebrate carrion decomposition. *J Med Entomol* 50(2):440–450
2. Michaud J-P, Moreau G (2009) Predicting the visitation of carcasses by carrion-related insects under different rates of degree-day accumulation. *For Sci Int* 185:78–83
3. Byrd JH, Allen JC (2001) The development of the black blow fly, *Phormia regina* (Meigen). *For Sci Int* 120(1–2):79–88
4. Byrd JH, Butler JF (1996) Effects of temperature on *Cochliomyia macellaria* (Diptera: Calliphoridae) development. *J Med Entomol* 33:901–905
5. Byrd JH, Butler JF (1997) Effects of Temperature on *Chrysomya rufifacies* (Diptera: Calliphoridae) development. *J Med Entomol* 34:353–358
6. Payne JA (1965) A summer carrion study of the baby pig *Sus scrofa* Linnaeus. *Ecology* 46(5):592–602
7. Schoenly K, Reid W (1987) Dynamics of heterotrophic succession in carrion arthropod assemblages: discrete seres or a continuum of change? *Oecologia* 73:192–202
8. Amendt J, Campobasso CP, Gaudry E, Reiter C, LeBlanc HN, Hall MJR (2007) Best practice in forensic entomology—standards and guidelines. *Int J Legal Med* 121(2):90–104
9. Byrd JH, Castner JL (2001) Forensic entomology: the utility of arthropods in legal investigations. CRC Press, Boca Raton, Florida
10. Villet MH (2011) African carrion ecosystems and their insect communities in relation to forensic entomology. *Pest Technol* 5(1):1–15
11. Greenberg B (1991) Flies as forensic indicators. *J Med Entomol* 28:565–577

12. Zimmerman KA, Wallace JR (2008) The potential to determine a postmortem submersion interval based on algal/diatom diversity on decomposing mammalian carcasses in brackish ponds in Delaware. *J For Sci* 53(4):935–941
13. Dickson GC, Poulter RTM, Maas EW, Probert PK, Kieser JA (2011) Marine bacterial succession as a potential indicator of postmortem submersion interval. *For Sci Int* 209(1–3):1–10
14. Hitosugi M, Ishii K, Yaguchi T, Chigusa Y, Kurosu A, Kido M, Nagai T, Tokudome S (2006) Fungi can be a useful forensic tool. *Legal Medicine* 8:240–242
15. Ronaghi M, Uhlén M, Nyrén P (1998) A sequencing method based on real-time pyrophosphate. *Science* 281(5375):363–365
16. Rothberg JM, Leamon JH (2008) The development and impact of 454 sequencing. *Nat Biotechnol* 26(10):1117–1124
17. Hudson ME (2008) Sequencing breakthroughs for genomic ecology and evolutionary biology. *Mol Ecol Resour* 8(1):3–17
18. Turnbaugh PJ, Quince C, Faith JJ, McHardy AC, Yatsunenko T, Niaz F, Affourtit J, Egholm M, Henrissat B, Knight R, Gordon JI (2010) Organismal, genetic, and transcriptional variation in the deeply sequenced gut microbiomes of identical twins. *Proc Natl Acad Sci U S A* 107(16):7503–7508
19. Edwards RA, Rodriguez-Brito B, Wegley L, Haynes M, Breitbart M, Peterson DM, Saar MO, Alexander S, Alexander EC, Rohwer F (2006) Using pyrosequencing to shed light on deep mine microbial ecology. *BMC Genomics* 7(57):1–7
20. The Human Microbiome Jumpstart Reference Strains Consortium (2010) A catalog of reference genomes from the human microbiome. *Science* 328(5981):994–999
21. Mahowald MA, Rey FE, Seedorf H, Turnbaugh PJ, Fulton RS, Wollam A, Shah N, Wang C, Magrini V, Wilson RK, Cantarel BL, Coutinho PM, Henrissat B, Crock LW, Russell A, Verberkmoes NC, Hettich RL, Gordon JI (2009) Characterizing a model human gut microbiota composed of members of its two dominant bacterial phyla. *Proc Natl Acad Sci U S A* 106:5859–5864
22. Price LB, Liu CM, Melendez JH, Frankel YM, Engelthaler D, Aziz M, Bowers J, Ratray R, Ravel J, Kingsley C, Keim PS, Lazarus GS, Zenilman JM (2009) Community analysis of chronic wound bacteria using 16S rRNA gene-based pyrosequencing: impact of diabetes and antibiotics on chronic wound microbiota. *PLoS One* 4(7):e6462
23. Petrosino JF, Highlander S, Luna RA, Gibbs RA, Versalovic J (2009) Metagenomic pyrosequencing and microbial identification. *Clin Chem* 55(5):856–866
24. Costello EK, Lauber CL, Hamady M, Fierer N, Gordon JI, Knight R (2009) Bacterial community variation in human body habitats across space and time. *Science* 326(5960):1694–1697
25. Schoenly KG, Haskell NH, Hall RD, Gbur JR (2007) Comparative performance and complementarity of four sampling methods and arthropod preference tests from human and porcine remains at the forensic anthropology center in Knoxville, Tennessee. *J Med Entomol* 44(5):881–894
26. Lewis AJ, Benbow ME (2011) When entomological evidence crawls away: *Phormia regina en masse* larval dispersal. *J Med Entomol* 48(6):1112–1119
27. Megyesi MS, Nawrocki SP, Haskell NH (2005) Using accumulated degree-days to estimate the postmortem interval from decomposed human remains. *J For Sci* 50(3):618–626
28. Michaud JP, Moreau G (2011) A statistical approach based on accumulated degree-days to predict decomposition-related processes in forensic studies. *J For Sci* 56(1):229–232
29. Catts EP (1992) Problems in estimating the postmortem interval in death investigations. *J Agric Entomol* 9(4):245–255
30. Dowd SE, Wolcott RD, Sun Y, McKeenhan T, Smith E, Rhoads D (2008) Polymicrobial nature of chronic diabetic foot ulcer biofilm infections determined using bacterial tag encoded FLX amplicon pyrosequencing (bTEFAP). *PLoS One* 3(10):e3326
31. Sen R, Ishak HD, Estrada D, Dowd SE, Hong E, Mueller UG (2009) Generalized antifungal activity and 454-screening of *Pseudonocardia* and *Amycolatopsis* bacteria in nests of fungus-growing ants. *Proc Natl Acad Sci U S A* 106(42):17805–17810
32. Handl S, Dowd SE, Garcia-Mazcorro JF, Steiner JM, Suchodolski JS (2011) Massive parallel 16S rRNA gene pyrosequencing reveals highly diverse fecal bacterial and fungal communities in healthy dogs and cats. *FEMS Microbiol Ecol* 76(2):301–310
33. Andreotti R, Perez de Leon AA, Dowd SE, Guerrero FD, Bendele KG, Scoles GA (2011) Assessment of bacterial diversity in the cattle tick *Rhipicephalus (Boophilus) microplus* through tag-encoded pyrosequencing. *BMC Microbiol* 11(1):1–6
34. Gontcharova V, Youn E, Wolcott RD, Hollister EB, Gentry TJ, Dowd SE (2010) Black Box Chimera Check (B2C2): a Windows-based software for batch depletion of chimeras from bacterial 16S rRNA gene datasets. *Open Microbiol J* 4:6
35. Dowd SE, Callaway TR, Wolcott RD, Sun Y, McKeenhan T, Hagevoort RG, Edrington TS (2008) Evaluation of the bacterial diversity in the feces of cattle using 16S rDNA bacterial tag-encoded FLX amplicon pyrosequencing (bTEFAP). *BMC Microbiol* 8:125
36. Wolcott RD, Gontcharova V, Sun Y, Dowd SE (2009) Evaluation of the bacterial diversity among and within individual venous leg ulcers using bacterial tag-encoded FLX and titanium amplicon pyrosequencing and metagenomic approaches. *BMC Microbiol* 9:226
37. Suchodolski JS, Dowd SE, Westermarck E, Steiner JM, Wolcott RD, Spillmann T, Harmoinen JA (2009) The effect of the macrolide antibiotic tylosin on microbial diversity in the canine small intestine as demonstrated by massive parallel 16S rRNA gene sequencing. *BMC Microbiol* 9:210
38. Li W, Dowd SE, Scurlock B, Acosta-Martinez V, Lyte M (2009) Memory and learning behavior in mice is temporally associated with diet-induced alterations in gut bacteria. *Physiol Behav* 96(4–5):557–567
39. Ishak HD, Plowes R, Sen R, Kellner K, Meyer E, Estrada DA, Dowd SE, Mueller UG (2011) Bacterial diversity in *Solenopsis invicta* and *Solenopsis geminata* ant colonies characterized by 16S amplicon 454 pyrosequencing. *Microb Ecol* 61(4):821–831
40. Nawrocki E, Kolbe D, Eddy S (2009) Infernal 1.0: inference of RNA alignments. *Bioinformatics* 25:1335–1337
41. Nawrocki EP, Eddy SR (2007) Query-dependent banding (QBD) for faster RNA similarity searches. *PLoS Comput Biol* 3:540–554
42. Garrity GM, Bell JA, Lilburn TG (2004) Taxonomic outline of the prokaryotes. In: Garrity GM (ed) *Bergey's manual of systematic bacteriology*, vol 2, 2nd edn. Springer, New York, New York, pp 4–23
43. Wang Q, Garrity GM, Tiedje JM, Cole JR (2007) Naïve Bayesian classifier for rapid assignment of rRNA sequences into the new bacterial taxonomy. *Appl Environ Microbiol* 73:5261–5267
44. R Development Core Team (2010) R: a language and environment for statistical computing. Vienna, Austria ISBN 3-900051-07-0: <http://www.R-project.org>
45. Anderson MJ (2001) A new method for non-parametric multivariate analysis of variance. *Austral Ecol* 26(1):32–46
46. McCune B, Mefford MJ (2006) PC-ORD
47. McCune B, Grace JB (2002) Analysis of ecological communities. MjM Software Design, Gleneden Beach, Oregon
48. Biondini ME, Bonham CD, Redente EF (1985) Secondary successional patterns in a sagebrush (*Artemisia tridentata*) community as they relate to soil disturbance and soil biological activity. *Vegetation* 60(1):25–36
49. Hastie T, Tibshirani R (1990) Generalized additive models. Chapman and Hall/CRC, Boca Raton
50. Panikov NS, Sizova MV (2007) Growth kinetics of microorganisms isolated from Alaskan soil and permafrost in solid media frozen down to –35 °C. *FEMS Microbiol Ecol* 59(2):500–512



51. Prescott LM, Harley JP, Klein DA (2004) Microbiology. 6th edition edn. McGraw-Hill Science/Engineering/Math.
52. Byrd JH, Castner JL (2010) Insects of forensic importance. In: Byrd JH, Castner JL (eds) Forensic entomology: the utility of arthropods in legal investigations, 2nd edn. CRC Press, Boca Raton, Florida, pp 39–126
53. Wilson EE, Wolkovich EM (2011) Scavenging: how carnivores and carrion structure communities. Trends Ecol Evol 26(3):129–135
54. Stadler S, Stefanuto P-H, Brokl M, Forbes SL, Focant J-F (2012) Characterization of volatile organic compounds from human analogue decomposition using thermal desorption coupled to comprehensive two-dimensional gas chromatography—time-of-flight mass spectrometry. Anal Chem 85(2):998–1005
55. Dekeirsschietier J, Verheggen FJ, Gohy M, Hubrecht F, Bourguignon L, Lognay G, Haubruge E (2009) Cadaveric volatile organic compounds released by decaying pig carcasses (*Sus domesticus* L.) in different biotopes. Forensic Science International 189(1-3):46–53
56. Grice EA, Kong HH, Renaud G, Young AC, Bouffard GG, Blakesley RW, Wolfsberg TG, Turner ML, Segre JA, NISC Comparative Sequencing Program (2008) A diversity profile of the human skin microbiota. Genome Res 18(7):1043–1050
57. Sibley C, Church D, Surette M, Dowd S, Parkins M (2012) Pyrosequencing reveals the complex polymicrobial nature of invasive pyogenic infections: microbial constituents of empyema, liver abscess, and intracerebral abscess. European Journal of Clinical Microbiology & Infectious Diseases 31(10):2679–2691
58. Ursell LK, Clemente JC, Rideout JR, Gevers D, Caporaso JG, Knight R (2012) The interpersonal and intrapersonal diversity of human-associated microbiota in key body sites. J Allerg Clin Immunol 129(5):1204–1208
59. Dewhirst FE, Chen T, Izard J, Paster BJ, Tanner ACR, Yu W-H, Lakshmanan A, Wade WG (2010) The human oral microbiome. J Bacteriol 192(19):5002–5017
60. Carter DO, Tibbett M (2003) Taphonomic mycota: fungi with forensic potential. J For Sci 48(1):168–171
61. Mille-Lindblom C, Fischer H, Tranvik LJ (2006) Antagonism between bacteria and fungi: substrate competition and a possible tradeoff between fungal growth and tolerance towards bacteria. Oikos 113(2):233–242
62. Boer W, Folman LB, Summerbell RC, Boddy L (2006) Living in a fungal world: impact of fungi on soil bacterial niche development. FEMS Microbiol Rev 29(4):795–811
63. Ferrandon D, Imler J-L, Hetru C, Hoffmann JA (2007) The *Drosophila* systemic immune response: sensing and signalling during bacterial and fungal infections. Nat Rev Immunol 7(11):862–874
64. Gottar M, Gobert V, Michel T, Belvin M, Duyk G, Hoffmann JA, Ferrandon D, Royet J (2002) The *Drosophila* immune response against Gram-negative bacteria is mediated by a peptidoglycan recognition protein. Nature 416(6881):640–644
65. Gerardo NM, Altincicek B, Anselme C, Atamian H, Barribeau SM, Md V, Duncan EJ, Evans JD, Gabaldón T, Ghanim M, Heddi A, Kaloshian I, Latorre A, Moya A, Nakabachi A, Parker BJ, Pérez-Brocail V, Pignatelli M, Rahbé Y, Ramsey JS, Spragg CJ, Tamames J, Tamarit D, Tamborindeguy C, Vincent-Monegat C, Vilcinskas A (2010) Immunity and other defenses in pea aphids. *Acyrtosiphon pisum* Genome Biol 11:R21
66. Wilson-Rich N, Spivak M, Fefferman NH, Starks PT (2009) Genetic, individual, and group facilitation of disease resistance in insect societies. Annual Rev Entomol 54:405–423
67. Suwannapong G, Benbow M, Nieh J (2011) Biology of Thai honeybees: natural history and threats. In: Florio R (ed) Bees: biology, threats and colonies. Nova Science Publishers, Inc, Hauppauge, NY, pp 1–101
68. Rozen DE, Engelmoer DJP, Smiseth PT (2008) Antimicrobial strategies in burying beetles breeding on carrion. Proc Natl Acad Sci U S A 105(46):17890–17895
69. Kerridge A, Lappin-Scott H, Stevens JR (2005) Antibacterial properties of larval secretions of the blowfly, *Lucilia sericata*. Med Vet Entomol 19:333–337
70. Nigam Y, Bexfield A, Thomas S, Ratcliffe NA (2006) Maggot therapy: the science and implication for CAM—Part II—maggots combat infection. Evidence-Based Complement Alter Med 3(3):303–308
71. Sherman RA, Hall MJR, Thomas S (2000) Medicinal maggots: an ancient remedy for some contemporary afflictions. Ann Rev Entomol 45(1):55–81
72. Mumcuoglu KY, Miller J, Mumcuoglu M, Friger M, Tarshis M (2001) Destruction of bacteria in the digestive tract of the maggot of *Lucilia sericata* (Diptera: Calliphoridae). J Med Entomol 38(2):161–166
73. Tomberlin JK, Crippen TL, Tarone AM, Singh B, Adams K, Rezenom YH, Benbow ME, Flores M, Longnecker M, Pechal JL, Russell DH, Beier RC, Wood TK (2012) Interkingdom responses of flies to bacteria mediated by fly physiology and bacterial quorum sensing. Anim Behav 84(6):1449–1456
74. Ma Q, Fonseca A, Liu W, Fields AT, Pimsler ML, Spindola AF, Tarone AM, Crippen TL, Tomberlin JK, Wood TK (2012) *Proteus mirabilis* interkingdom swarming signals attract blow flies. The ISME Journal:1–11
75. Ieno EN, Amendt J, Fremdt H, Saveliev AA, Zuur AF (2010) Analysing forensic entomology data using additive mixed effects modelling. In: Current Concepts in Forensic Entomology. Springer, Dordrecht, pp 139–162. ISBN 978-1-4020-9683-9
76. Tarone AM, Foran DR (2008) Generalized additive models and *Lucilia sericata* growth: assessing confidence intervals and error rates in forensic entomology. J For Sci 53(4):942–948
77. Wells J, LaMotte LR (1995) Estimating maggot age from weight using inverse prediction. J For Sci 40:585–585
78. Clark K, Evans L, Wall R (2006) Growth rates of the blowfly, *Lucilia sericata*, on different body tissues. For Sci Int 156(2–3):145–149
79. Donovan SE, Hall MJR, Turner BD, Moncrieff CB (2006) Larval growth rates of the blowfly, *Calliphora vicina*, over a range of temperatures. Med Vet Entomol 20(1):106–114
80. Nability PD, Higley LG, Heng-Moss TM (2006) Effects of temperature on development of *Phormia regina* (Diptera: Calliphoridae) and use of developmental data in determining time intervals in forensic entomology. J Med Entomol 43(6):1276–1286
81. Tarone AM, Foran DR (2011) Gene Expression During Blow Fly Development: Improving the Precision of Age Estimates in Forensic Entomology. J For Sci 56:S112–S122
82. Michaud JP, Majka CG, Prive JP, Moreau G (2010) Natural and anthropogenic changes in the insect fauna associated with carcasses in the North American Maritime lowlands. Forensic Sci Int 202(1–3):64–70
83. Shendure J, Ji H (2008) Next-generation DNA sequencing. Nat Biotechnol 26(10):1135–1145
84. Richards CS, Villet MH (2009) Data quality in thermal summation development models for forensically important blowflies. Med Vet Entomol 23(3):269–276
85. Richards C, Paterson I, Villet M (2008) Estimating the age of immature *Chrysomya albiceps* (Diptera: Calliphoridae), correcting for temperature and geographical latitude. Int J Legal Med 122(4):271–279
86. Boatright SA, Tomberlin JK (2010) Effects of temperature and tissue type of *Cochliomyia macellaria* (Diptera: Calliphoridae). Journal of Medical Entomology 37(5):917–923